ELSEVIER

Journal of Hydrology 272 (2003) 276–290

Journal of Hydrology

www.elsevier.com/locate/jhydrol

Multiresolution analysis of data on electrical conductivity of soil using wavelets

R.M. Lark[a,*], S.R. Kaffka[b], D.L. Corwin[c]

[a]*Math and Decision Systems Group, Silsoe Research Institute, Wrest Park, Silsoe, Bedford MK45 4HS, UK*
[b]*Department of Agronomy and Range Science, University of California, Davis, CA 95616, USA*
[c]*ARS, USDA, George E. Brown, Jr. Salinity Laboratory, 450 W Big Springs Rd, Riverside, CA 92507, USA*

Abstract

The variation of soil properties at the field scale can be complex. Particular challenges for the analysis of data on soil variables arise when components of variation operate at a range of scales, show intermittent effects, and are not spatially stationary in the variance, fluctuating more in some regions than in others.

Wavelet analysis addresses these problems. Any data set of finite variance (appropriately sampled) may be analysed with the dilations and translations of a basic wavelet function. Wavelet functions oscillate locally and damp rapidly to zero either side of their centre, so that they only respond to variation within a local neighbourhood. To provide a complete analysis of a data set the wavelet must be translated across the data, generating a set of local coefficients. The basic wavelet can also be dilated to analyse the data at a specified spatial scale. A single wavelet coefficient therefore describes the variation of a variable in some locality at a particular spatial scale.

Data were collected at a variable, 32.4 ha salt affected site in the Tulare Lake Bed region of California using electrical conductivity sensors (mobile fixed-array, electrical resistivity equipment). We show how wavelets can be used to analyse the variation within these data, how the analysis partitions the variance of the data by scale and location, and how it can be used to extract components from the data which appear to be more useful for predicting soil properties than are the raw data.
© 2002 Elsevier Science B.V. All rights reserved.

Keywords: Wavelets; Geostatistics; Soil; Salinity; Electrical conductivity

1. Introduction

Environmental variables typically show substantial variation over a wide range of spatial scales. This variability is a challenge for modelling environmental processes or characterising them by sampling in space. In the face of such complexity we require a method for the analysis of variation. One approach, which has been successful for many problems, is to treat data on an environmental variable as realizations of a stochastic process. Some assumptions are usually necessary, notably that the variance of the process is constant (stationary) in space. The assumption of the intrinsic hypothesis, that the expected variance of the difference between values of the process at two locations depends only on their separation in space, underlies most geostatistical analysis (Webster and Oliver, 2001). If this assumption is plausible then it provides a basis for estimating values of a variable from limited samples (Burgess and Webster, 1980),

* Corresponding author. Tel.: +44-1525-860000; fax: +44-1525-860156.
E-mail address: murray.lark@bbsrc.ac.uk (R.M. Lark).

0022-1694/03/$ - see front matter © 2002 Elsevier Science B.V. All rights reserved.
PII: S0022-1694(02)00271-8

for describing the correlation between two variables when this depends on spatial scale (Goovaerts and Webster, 1994) and for filtering the data into components of different spatial scale to aid interpretation (Oliver et al., 2000).

While geostatistics has been successful there are some kinds of variation to which it cannot be satisfactorily applied. The most serious problem is non-stationarity of the variance. This has been encountered in soil variables (Voltz and Webster, 1990) who found changes in the variance of soil pH and clay content on a transect across Jurassic sediments in Central England. It is for this reason that attention has been directed to alternative methods of analysis which make less restrictive assumptions about the nature of variability.

One approach, within the sphere of geostatistics, is to conduct conventional geostatistical analyses in a moving window, within which the assumption of the intrinsic hypothesis is more plausible (Walter et al., 2001). Another method is wavelet analysis, which is the focus of this paper. Wavelet analysis, described more fully below, uses wavelets and corresponding scaling functions as basis functions to decompose a set of data into components described by wavelet coefficients. These coefficients are specific to spatial scales and locations. Analysis of the coefficients can therefore give insight into the variability of a property. Reconstituting data from subsets of the wavelet coefficients specific to different spatial scales allows us to generate representations of the data at different spatial resolution—so-called multiresolution analysis (MRA). Lark and Webster (1999) demonstrated how wavelet analysis could be used to analyse the complex variation of soil properties on the same transect where Voltz and Webster (1990) had questioned the intrinsic hypothesis. The wavelet analysis decomposed the soil variables into components of different spatial scale, some of which were clearly not of uniform variability in space. More recently Lark and Webster (2001) have shown how the location of changes in variance may be detected statistically using wavelet coefficients.

Wavelet analysis requires substantial numbers of regularly sampled data. This inevitably limits the scope for its application to environmental variables which must be measured directly by field sampling and laboratory analysis. For this reason Lark and Webster (2001) suggested that wavelet analysis might be most useful for the analysis of cheaper data obtained using sensors.

The measured bulk soil electrical conductivity (EC_a) is among the most useful and easily obtained spatial properties of soil that influence crop productivity (Corwin and Lesch, 2002). As a result, soil EC_a has become one of the most frequently used measurements to characterize field variability (Corwin and Lesch, 2002). EC_a may be measured with electrical resistivity where the electrodes make direct contact with the soil or may be measured non-invasively with electromagnetic inductance. Mobilized, fixed-array, electrical-resistivity and mobilized electromagnetic induction (EM) equipment have been developed that geo-references the EC_a measurement with GPS (Carter et al., 1993; McNeil, 1992; Rhoades, 1992, 1993). This equipment makes it possible to measure and map EC_a at field scales in real-time (Rhoades et al., 1999). Bulk soil electrical conductivity is influenced by physical and chemical properties of soil. These properties include soil salinity, clay content and cation exchange capacity, clay mineralogy, soil pore size and distribution, soil moisture content, organic matter, bulk density, and soil temperature (McNeil, 1992; Rhoades et al., 1999; Corwin and Lesch, 2002). EC_a may be used to predict values of these soil properties using, for example, regression models obtained from a few calibration data (Corwin and Lesch, 2002).

The goal of this paper is to demonstrate how MRA using wavelets may be applied to data on soils obtained from sensors of electrical conductivity. The analysis shows the complexity of the variation in these data at different spatial scales. We also evaluate the effect of filtering the data, by removing components of particular spatial scales, on their usefulness for predicting soil variables obtained by sampling and analysis.

2. Theory

We denote our data as a function of location in space, $f(x)$. It will be noted that this is a one-dimensional function, and in this paper the analysis is limited to one-dimension because of the nature of the data as discussed below. In principle wavelet analysis is not so limited. A basic or 'mother' wavelet may also

be defined as a function of location, $\psi(x)$. A wavelet function must have three properties: the mean is zero, i.e.

$$\int_{-\infty}^{\infty} \psi(x)\mathrm{d}x = 0, \tag{1}$$

the squared norm is 1, i.e.

$$\int |\psi(x)|^2 \, \mathrm{d}x = 1 \tag{2}$$

and the function has a compact support. This last condition means that the wavelet only takes non-zero values over a narrow interval. This property is illustrated by the so-called 'Mexican hat' wavelet function in Fig. 1a.

The wavelet transform is an integral transform, that is to say a wavelet coefficient is obtained by integrating the product of a wavelet with the data. It is clear that a wavelet coefficient, because of the compact support of the wavelet, will only respond to the data over a finite interval, and so gives a localized description of the data's variability. In order to analyse data over a transect it is necessary to shift the wavelet (translate it) as in Fig. 1b. Furthermore, the scale at which a wavelet coefficient describes the data may be changed by shrinking or dilating the wavelet function (Fig. 1c). For a basic wavelet function $\psi(u)$ a dilated and translated version $\psi_{\lambda,x}(u)$ may be obtained with the following equation:

$$\psi_{\lambda,x}(u) = \frac{1}{\sqrt{\lambda}}\psi\left(\frac{u-x}{\lambda}\right), \qquad \lambda > 0, \;\; x \in \Re, \tag{3}$$

$\Re$ denotes the set of real numbers. The parameter λ is the 'scale parameter' of the wavelet and controls its dilation. The parameter x determines the location of the wavelet.

The wavelet coefficient for scale parameter λ and location x, $Wf(\lambda, x)$ is defined as the integral

$$\begin{aligned} Wf(\lambda,x) &= \int_{-\infty}^{\infty} f(u)\psi_{\lambda,x}(u)\mathrm{d}u \\ &= \int_{-\infty}^{\infty} f(u)\frac{1}{\sqrt{\lambda}}\psi\left(\frac{u-x}{\lambda}\right). \end{aligned} \tag{4}$$

In principle the two parameters can be varied continuously, in practice they must be discretized, and in the discrete wavelet transform (DWT) this is done by setting λ to integer powers, m of a basic dilation step λ_0 where $\lambda_0 > 1$. Commonly $\lambda_0 = 2$ so the scale parameter increases in the dyadic sequence $\lambda_0^m = 2, 4, 8, \ldots$ The location is incremented in steps which depend on the scale parameter so that $x = nx_0\lambda_0^m$, where n is an integer and x_0 is a basic step (commonly one interval between samples on the transect). In the notation we denote a discretely scaled and translated wavelet function by $\psi_{m,n}$. The DWT coefficient is $D_{m,n}$ where

$$D_{m,n} = \langle f, \psi_{m,n}\rangle = \lambda_0^{-m/2}\int f(x)\psi(\lambda_0^{-m}x - nx_0)\mathrm{d}x. \tag{5}$$

The inner product of two vectors is denoted by putting them in the $\langle\,\rangle$ and f denotes our data.

A set of DWT functions, for wavelet functions with certain properties, provides a complete orthonormal basis for any data set of finite variance (Daubechies, 1988, 1992). In short this means that the resulting wavelet coefficients may be used to approximate the data to any degree of precision by the equation:

$$f(x) = \sum_{m=-\infty}^{\infty}\sum_{n=-\infty}^{\infty} D_{m,n}\psi_{m,n}(x). \tag{6}$$

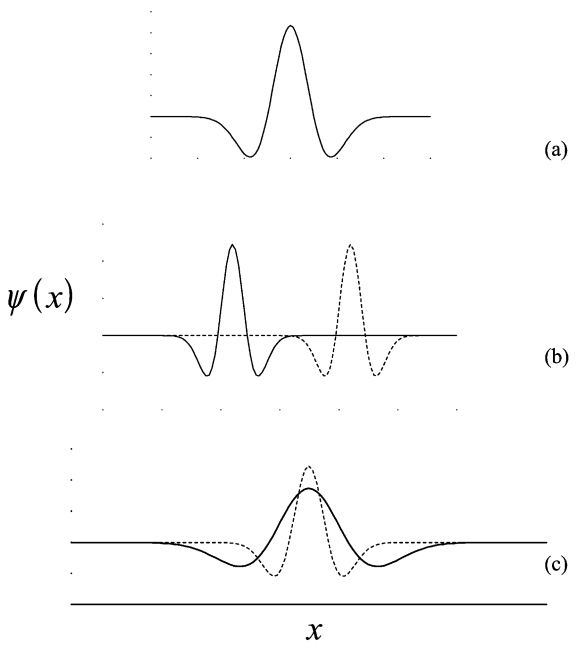

Fig. 1. (a) A basic wavelet function (Mexican Hat) with, (b) two translations and (c) two dilations.

This equation follows from the basic ideas of basis functions of vector spaces. More details can be found in the Appendix to Lark and Webster (1999).

Because the wavelet basis functions are orthogonal to their dilates and translates, if we evaluate the sum of products of the wavelets and their coefficients over all locations but for just one value of the scale parameter, 2^k then we obtain an additive component of the discretely sampled data. This is called the *detail component* for scale parameter 2^k, or $Q_k f(x)$, where

$$Q_k f(x) = \sum_{n=-\infty}^{\infty} D_{k,n}\psi_{k,n}(x). \tag{7}$$

One may imagine filtering the data $f(x)$ by removing these additive components for all values of the scale parameter 2^m, $m = 1, 2, \ldots, k$. The result is the so-called 'smooth' representation of the data for scale parameter 2^k, denoted $P_k f(x)$. It can be shown (Mallat, 1989) that the smooth representation may be obtained by

$$P_k f(x) = \sum_{n=-\infty}^{\infty} \langle f, \phi_{k,n}\rangle \phi_{k,n}(x) \tag{8}$$

where $\phi_{k,n}$ is a scaled and translated basis function called the scaling function. The scaling function bears a unique relationship to a particular wavelet function, and can be thought of as a smoothing kernel. A full account of how the scaling functions and wavelet functions are related is given by Lark and Webster (1999).

The discussion above outlines how a sequence of discretely sampled data might be partitioned into a set of detail components and a smooth representation using wavelets and the corresponding scaling functions. This decomposition is known as MRA.

Many wavelet functions can be used for MRA. Daubechies (1988) provides a widely used family of wavelet functions with the required properties to define an orthonormal basis. We may think of a particular dilation of the mother wavelet as defining a filter with which the data are convolved. The DWT coefficients are obtained by subsampling the output of this convolution at intervals of 2^m. This is most efficiently done using the Pyramid Algorithm (described clearly by Press et al. (1992)).

Since convolution underlies the DWT it is a problem to obtain coefficients near the ends of the data where the filter overlaps the first or the last data point. In some applications of wavelet analysis this may be solved by 'wrap-around' conditions, i.e. the data are assumed to lie on a circle, but this is not appropriate for spatial analysis. One solution, proposed by Cohen et al. (1993) is to use adapted filters near the ends of the transect. Lark and Webster (1999) used these adapted filters, but they have limitations, discussed by Lark and Webster (2001).

Another problem with the DWT, for some wavelet bases, is that it is not shift invariant—the value of a wavelet coefficient for a location will depend on where the analysis starts. Lark and Webster (1999) took up a proposal of Coifman and Donoho (1995) and computed a set of MRA advancing the starting point for each. Averaging the resulting components removed artefacts from the analysis.

When the wavelet function in a DWT meets certain criteria (Daubechies, 1992) then the DWT partitions the variance of a set of data over all scales. If $\mathrm{SS}_k f(x)$ denotes the sum-of-squares of $P_k f(x)$ and $\mathrm{SS} f(x)$ the sum-of-squares of $f(x)$ then

$$\mathrm{SS} f(x) = \mathrm{SS}_k f(x) + \sum_{m=1}^{k}\sum_{n=1}^{n_m} D_{m,n}^2 \tag{9}$$

where there are n_m DWT coefficients for scale parameter 2^m.

This is the basis of the sample wavelet variance (Percival, 1995), $\hat{\sigma}_k^2$, the contribution to the variance of the data made by components for scale parameter 2^k

$$\hat{\sigma}_k^2 = \frac{1}{2^k n_k}\sum_{n=1}^{n_k} D_{k,n}^2. \tag{10}$$

The wavelet variance defined in Eq. (10) is based on DWT coefficients, and so on a subsample of the convolution of the data with a filter. Percival and Guttorp (1994) showed that the wavelet variance could be more efficiently estimated by retaining all coefficients from the convolution. These are the maximal overlap DWT coefficients (MODWT). Lark and Webster (2001) used MODWT coefficients obtained with adapted filters at the ends of the data, adapted MODWT (AMODWT) coefficients, $\breve{d}_{k,n}$. There are N AMODWT coefficients for any scale parameter 2^k from a sequence of N data.

The AMODWT variance can be obtained as

$$\breve{\sigma}_k^2 = \frac{1}{2^k N} \sum_{n=1}^{N} \breve{d}_{k,n}^2. \quad (11)$$

Lark and Webster (2001) proposed discarding the first 2^k coefficients for $k = 1$ and $k = 2$ when using Cohen et al.'s (1993) adapted wavelets since these are particularly biased. When estimating $\breve{\sigma}_k^2$ for $k = 1$ or 2 using Eq. (11) the N in the divisor is replaced by $N - 2^k$ and the summation is conducted over the range $n = 2^k + 1, \ldots N$.

The wavelet variance is directly related to the power spectrum (Abry et al., 1995). As such it represents a partition of the variance of the data by scale (a frequency band) aggregated over all locations. In calculating wavelet variances we therefore discard by aggregation the information which wavelet coefficients, because of their localized reference, contain about changes in the variability of a variable which may occur with location. Lark and Webster (1999, 2001) showed that plots of the local contributions to wavelet variance, for example the AMODWT-based values

$$\frac{\breve{d}_{k,n}^2}{2^k}, \quad (12)$$

may be informative showing how, at different scale parameters, the variability of a property may change in space. Lark and Webster (2001) have shown how this visual interpretation may be developed into a quantitative methods for detecting scale-specific changes in variance within an inferential framework.

3. Materials and methods

The methods and materials that were used to conduct the EC_a survey followed the suggested guidelines of Corwin and Lesch (2002). GPS-based mobile electrical resistivity and EM equipment were used to measure and geo-reference EC_a at a 32.4 ha (80 acre) study site. The tractor-mounted, invasive fixed-array unit and the non-invasive mobile EM unit were developed by Rhoades and colleagues (Carter et al., 1993; Rhoades, 1992, 1993). The study site was located in California's San Joaquin Valley. The soil at the site was a Lethent clay loam (fine, montmorillanitic, thermic, typic Natrargid). These soils are saline-sodic, and have little organic matter. The study site was divided into 8 rectangular paddocks roughly 4 ha in area. The EC_a survey was conducted in August, 1999, on fallow soil prior to planting with Bermuda grass. The survey consisted of an initial cursory EM survey followed by an intensive fixed-array, electrical-resistivity EC_a survey. A total of 384 EM readings were taken. A total of 7288 electrical-resistivity EC_a measurements were taken. Each EC_a measurement was geo-referenced using GPS. The initial survey consisted of a grid of EC_a measurements taken with the mobile EM equipment. The grid was arranged in a 4×12 pattern within each of the eight paddocks. At each site, both horizontal and vertical EM measurements were taken. The horizontal coil configuration results in a measurement EM_h that concentrates the reading nearer to the soil surface and penetrates to a depth of approximately 1 m, whereas the reading in the vertical configuration, EM_v penetrates to a depth of 1.5 m and concentrates the reading less at the surface. The geometric mean EM levels were defined as $\sqrt{EM_v EM_h}$. The profile ratios were defined as EM_h/EM_v. The profile ratio provided an indication of the shape of the EC_a profile (regular, inverted or uniform). Profile ratios equal to 1 indicate a uniform profile, profile ratios <1 indicate an increasing profile with depth, and profile ratios >1 indicate an inverted profile (i.e. conductivity decreases with depth). In essence, the profile ratio is analogous to the leaching fraction, while the geometric mean approximates the relative level of salinity in the root zone. Using the EM data from the initial cursory survey and statistical software (ESAPv2.0) developed by Lesch et al. (1995), five sites within each paddock (40 total) were selected that characterize the spatial variability in EC_a across each paddock. The first four sample locations of each paddock were selected so that one location satisfied each of the following four criteria: (i) high geometric mean EM and high profile ratio, (ii) high geometric mean EM and low profile ratio, (iii) low geometric mean EM and high profile ratio, and (iv) low geometric mean EM and low profile ratio. The fifth sample site was chosen randomly within each paddock. The highs and lows were identified in each paddock on a paddock-by-paddock basis. Another statistical criterion for

the selection of each site was the minimization of spatial clustering. At each of these 40 sites, soil core samples were taken at two points roughly 5 cm apart. Soil cores were taken at 0.3 m increments to a depth of 1.2 m. These cores were analysed for a variety of physical and chemical properties related to soil quality. Among some the properties analysed were bulk density (ρ), volumetric water content (θ), and electrical conductivity of the saturation extract (EC_e). Complete analytical results are reported in Corwin et al. (2002). The fixed-array, electrical-resistivity electrodes were set to determine EC_a to a depth of 1.2 m. The data were collected on 80 passes east-to-west across the field, EC_a measurements were taken at 4 m intervals. The data were therefore closer together east–west than north–south, and the north–south spacing of the passes was not entirely regular. This precludes a two-dimensional wavelet analysis so the following one-dimensional analyses, as described in Section 2, were conducted on each pass.

1. MRA was done using Cohen et al.'s (1993) adaptation of Daubechies' (1988) wavelet with two vanishing moments. The Shift-averaging procedure of Lark and Webster (1999) was used. This generated average detail components for scale parameter $x_0 2^m$ where x_0, the basic step, is the 4 m interval along the pass and $m = 1, 2, \ldots, 4$, with a smooth component for the coarsest scale $x_0 2^4 = 64$ m. Below we refer to the scale parameter in terms of the dyadic sequence of multipliers of the basic step (i.e. 2^m), where necessary reminding the reader of the value of the scale parameter in metres.
2. AMODWT coefficients were computed for scale parameters 2, 4, 8 and 16 using the AMODWT transform of Lark and Webster (2001). The AMODWT coefficients were used to compute wavelet variances—Eq. (11)—for all scales on two selected passes and an average over all passes. The local contributions to the wavelet variances—Eq. (12)—were also calculated.
3. The variation of EC_a on the two selected passes was tested for uniformity at each scale parameter. This was done following the work of Whitcher et al. (2000) and Lark and Webster (2001), by computing a normalized sum-of-squares statistic, $S_{k,r}$, which is a function of location r and specific to scale parameter 2^k

$$S_{k,r} = \frac{1}{2^k N \breve{\sigma}_k^2} \sum_{n=1}^{r} \breve{d}_{k,n}^2. \tag{13}$$

The normalising term in front of the summation simply scales the statistic to a maximum value of 1. Under an assumption of uniform variance at scale parameter 2^k $S_{k,r}$ is expected to increase linearly from 0 to 1. If there is a change in variance at this scale at one or more locations then the plot of $S_{k,r}$ will change slope at these locations. The location r' for which $S_{k,r}$ deviates most from the bisector is the first candidate location for a change in variance at scale parameter 2^k. The wavelet variances may be computed for the two segments either side of location r' and the variance ratio computed. Because of the complex and scale-dependent correlations among the AMODWT coefficients a Monte Carlo method was used by Lark and Webster (2001) to compute percentage points of the wavelet variance ratio under a null hypothesis that the variance of the underlying process is stationary. The same procedure was used here to test the evidence for a change in variance at the first candidate change point for each scale parameter.

The EC_a data and the smooth and detail components from the MRA were extracted at each of the 40 sites where the soil has been sampled for analysis. The soil properties at each depth were then regressed on (i) the raw EC_a data, (ii) the smooth representation at scale parameter 2^3 (32 m), (iii) the smooth representation at scale parameter 2^4 (64 m) and (iv) the smooth representation at scale parameter 2^4 (64 m) and the detail component for this scale parameter as a separate predictor. Note that the sum of the two predictors in (iv) is equal to the predictor in (iii). The regression was done by a model-based Maximum likelihood method described elsewhere by Lark (2000) based on the work of Cook and Pocock (1983). In summary, estimates of the n regression coefficients for m observations of n predictor variables are contained in the vector $\mathbf{b}$ where

$$\mathbf{b} = (\mathbf{X}^{\mathrm{T}}\mathbf{A}^{-1}\mathbf{X})^{-1}(\mathbf{X}^{\mathrm{T}}\mathbf{A}^{-1}\mathbf{y}), \tag{14}$$

where $\mathbf{A}$ is the $m \times m$ matrix of autocorrelations among the errors. $\mathbf{X}$ is an $n \times m$ matrix of values of the n predictors and the vector $\mathbf{y}$ contains the n observed values of the soil property. The error

variance is estimated by

$$\hat{\sigma}^2 = \frac{1}{n}(\mathbf{y} - \mathbf{Xb})^{\mathrm{T}}\mathbf{A}^{-1}(\mathbf{y} - \mathbf{Xb}). \quad (15)$$

In order to evaluate these two expressions the matrix **A** is needed. It may be defined with reference to the parameters of a variogram model, specifically the distance parameter and the ratio of the nugget to the sill variance. This entails the assumption that the autocorrelation of the errors of the regression model at locations $\mathbf{x}_i$ and $\mathbf{x}_j$ depends only on the vector $\mathbf{x}_i - \mathbf{x}_j$. The maximum likelihood regression is fitted by finding the variogram parameters which maximize the log-likelihood term

$$-\log|\mathbf{A}| - n \log \hat{\sigma}^2. \quad (16)$$

This must be done numerically.

The inference of the significance of the regression model was based on the Wald statistic. In order to compare models with different numbers of predictors the variable portion of the Akaike Information criterion was computed

$$a = \log|\mathbf{A}| + n \log \hat{\sigma}^2 + 2P, \quad (17)$$

where P is the number of predictors in the model. If adding extra predictors to a model (which increases the term $2P$) reduces the value of a (due to the reduction in $\hat{\sigma}^2$) then this is evidence that the additional predictors add information to the model which justifies its extra complexity.

4. Results

Fig. 2 shows the histogram of EC_a data. These are more or less symmetrically distributed with a coefficient of skew of only -0.13. It was found that log-transformation of the raw EC_a data reduced their correlation with the observed soil properties at most depths. Given these two observations we worked with the EC_a data in their original units (dS m^{-1}).

Fig. 3 is a post-plot of the raw EC_a data and Fig. 4 is a corresponding plot of the smooth representations generated by the MRA for four scales. The corresponding detail components are shown in Fig. 5.

Fig. 6 shows the overall wavelet variances from the whole field for each scale parameter. The individual contributions to this variance from locations across the field—Eq. (12)—are shown in Fig. 7. Note that these are square-root transformed back to units of conductivity.

The overall partition of variance in EC_a between the spatial scales appears to be more or less uniform, but the results of the wavelet analyses make it clear that this conceals a complex pattern of spatial variability. Fig. 7 shows that there is considerable heterogeneity in the contributions to variation, particularly at the three finest scales where the north-eastern corner of the site shows much greater variation than does the rest of the site. The detailed examination of pass 2 (second from the bottom on the plots) and the northernmost pass 80 confirm this. Fig. 8 shows the wavelet variances for these two passes. Pass 80 is more variable than the average for scale parameter 2–8 (8–32 m). Pass 2 is less variable than average at the two finest scales. Both passes show similar variance at the coarsest scale and the confidence intervals for the wavelet variances both overlap the average value for the whole site.

Within both passes the variability changes, as is seen in Fig. 9 which shows the contributions to wavelet variance at each location and scale parameter. Fig. 10 shows the data and the smooth representation at scale parameter 16 (64 m) and Fig. 11 shows the detail components for each scale parameter.

Table 1 shows that significant changes in variance can be detected in both passes at the three finer spatial scales. It should be noted that the two segments identified by this procedure at any scale could be investigated for further changes in variance. This complex variability is not surprising. Soil

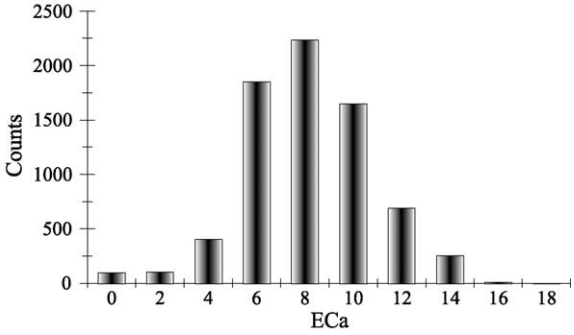

Fig. 2. Histogram of EC_a data (dS m^{-1}).

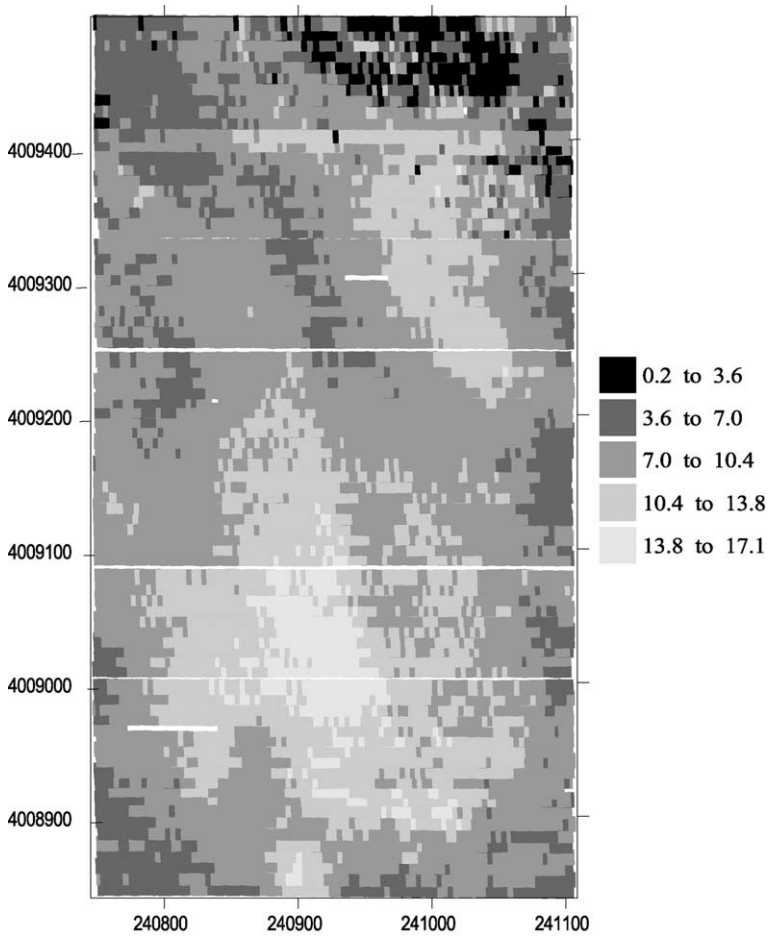

Fig. 3. EC_a data (dS m^{-1}) for the site.

conductivity will be influenced by many properties of the soil which may be complex and non-stationary in their effects.

The extreme heterogeneity in the northeast corner is due to contact problems between the four fixed-array electrodes and the soil. The soil in the northeast corner was extremely dry in the top 15–22 cm. This dryness was highly variable across the soil surface. Because of this dryness, the electrodes would sporadically lose electrical contact with the soil as reflected by EC_a measurements falling near or below 0.1 dS m^{-1}. Ideally, EC_a measurements with invasive electrical-resistivity equipment should always to taken with the soil at field capacity to insure good contact, but in this instance that was not possible. It is notable that the contrast between this corner and the rest of the field is most pronounced at the finest spatial scale.

These results cast some doubt on the assumption of intrinsic stationarity which would be made in geostatistical analysis of these data by kriging or cokriging. The intrinsic hypothesis includes the second-order assumption that a variogram $\gamma(\mathbf{h})$ exists,

$$\mathrm{E}\{Z(\mathbf{x}) - Z(\mathbf{x}+\mathbf{h})\}^2] = \gamma(\mathbf{h}), \tag{18}$$

which depends only on the lag vector $\mathbf{h}$ and not on the location vector $\mathbf{x}$ where $Z(\mathbf{x})$ is the random function invoked in geostatistics as an abstract process of which the observed data are assumed to be a realization. Clearly the changes detected in the variance here give rise to doubts about

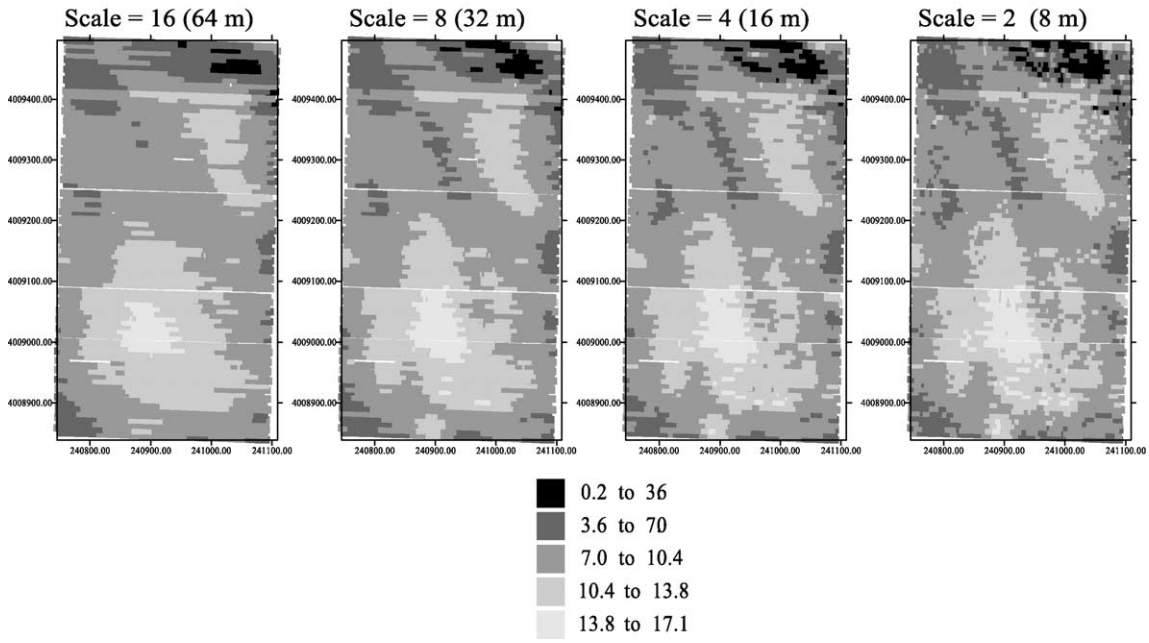

Fig. 4. Smooth representation of EC_a data from one-dimensional wavelet transforms.

the assumptions of geostatistics. While the kriged estimates of a variable are unlikely to be much affected by non-stationarity of the variance, the kriging variances are likely to be misleading.

The results of the regression analysis, shown in Table 2, are interesting. With the exception of the θ at one depth, the best predictors of soil variables are the variables generated by the MRA. In the case of

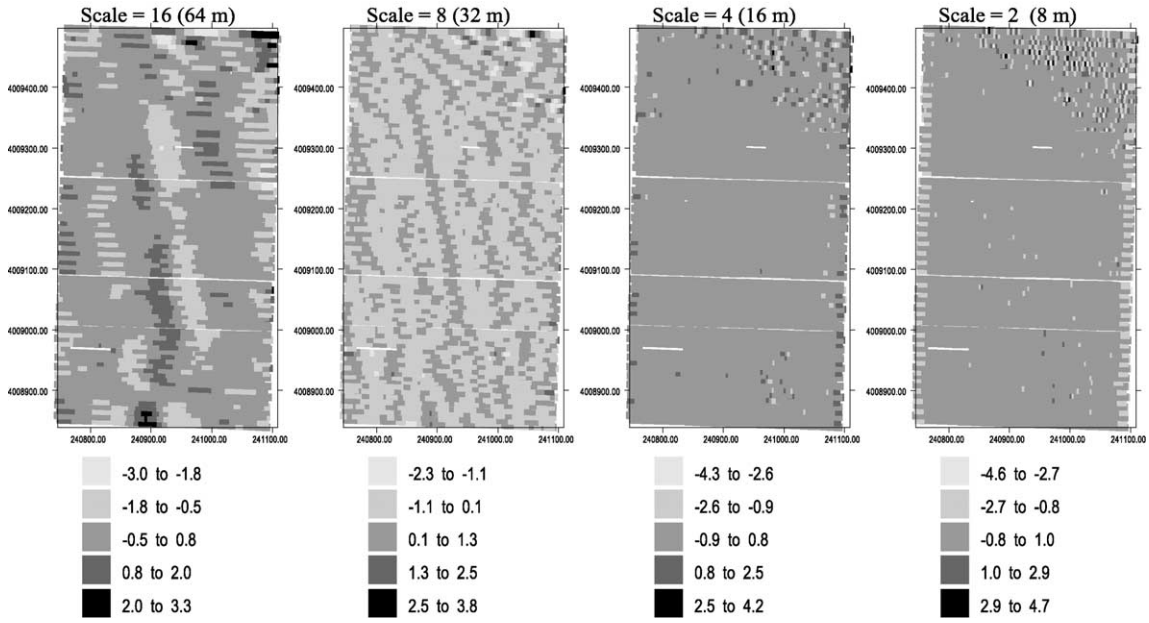

Fig. 5. Detail components of EC_a data from one-dimensional wavelet transforms.

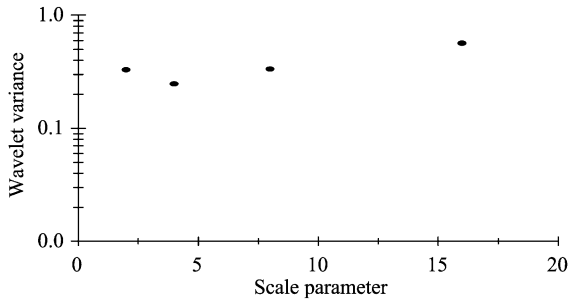

Fig. 6. Overall wavelet variances from the whole field for each scale parameter.

the variable EC_e the reduction in the error variance on using the smooth components can be quite substantial, particularly at depth. This implies that the finer scale components of the EC_a data may be regarded as noise for the purpose of predicting this soil property. Where using the detail component (scale parameter 16 (64 m) and the smooth component at this scale as separate predictors gives an improvement in the fit of the model over using the smooth representation at scale 8 (32 m) as a single predictor (e.g. for EC_e at 30 or 120 cm), this implies a difference in the information about this soil property contained in different scale components of the EC_a data.

5. Discussion and conclusions

These results have practical implications. First, they show that the information about soil properties contained in a signal from a sensor is not necessarily equally distributed among the spatial scales. Decomposing the signal into components of different spatial scale may improve the predictive value of the sensor data, since the different spatial scales may then be weighted differently. Second, the results call into question any approach to the analysis of such data which assumes that they are generated by a spatially stationary process. So, for example, to use raw EC_a data for co-kriging soil properties might be of

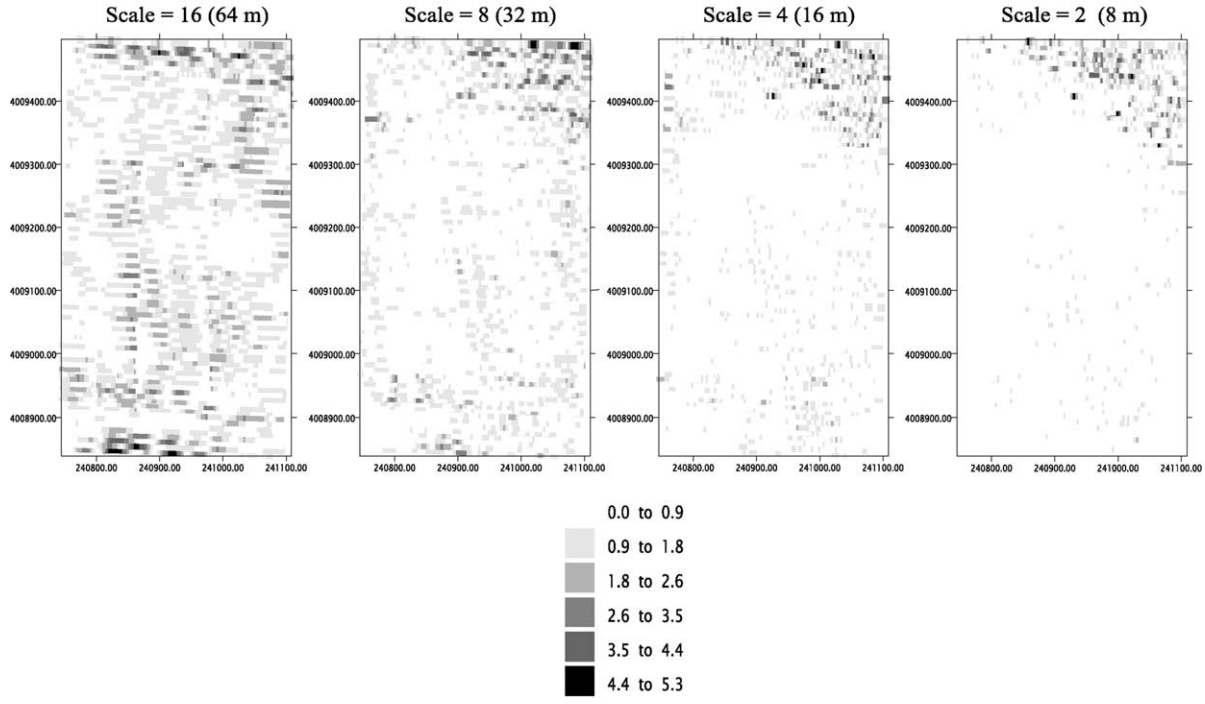

Fig. 7. Components of the wavelet variance (square-root transformed) for each scale parameter.

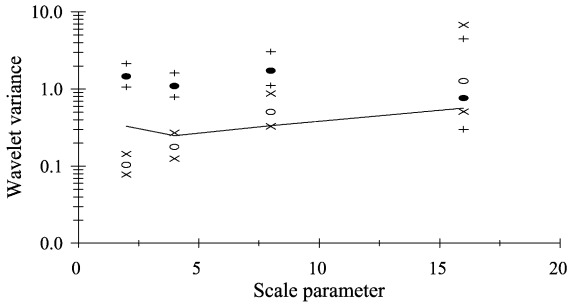

Fig. 8. Wavelet variances for two passes. Solid circle and crosses—sample wavelet variances for pass 80 and 95% confidence limits. Open circle and crosses—sample wavelet variances for pass 2 and 95% confidence limits. Line—wavelet variances for the whole data set.

questionable value. A better procedure would be first to filter out those components at finer scale which appear to be noise (from the perspective of predicting soil properties) then to use the resulting smooth representation of the data either to predict the soil properties by regression, or as an external drift

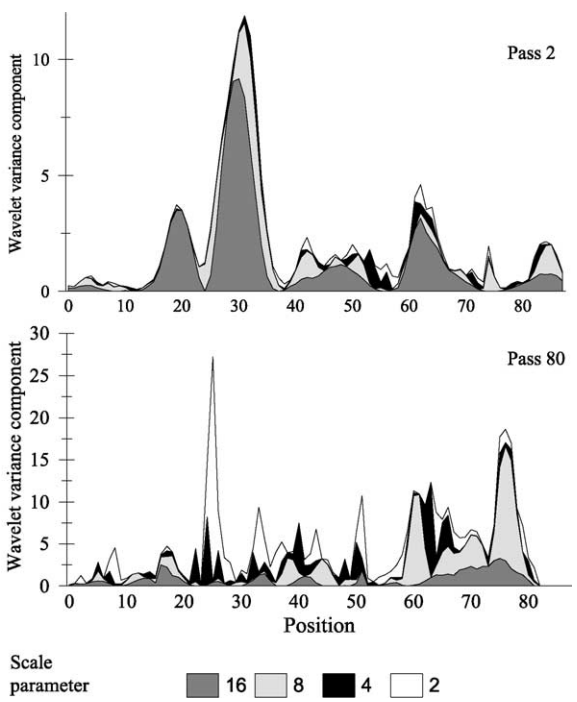

Fig. 9. Contributions to wavelet variance at each scale parameter at locations on two passes.

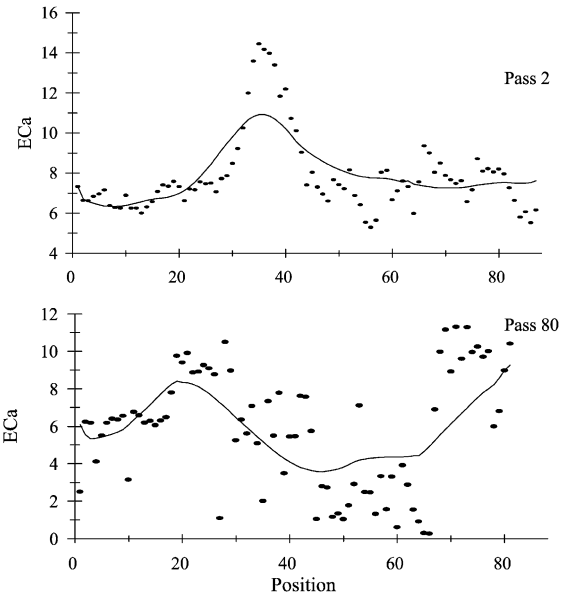

Fig. 10. Data (symbols) and the smooth representation (line) at scale parameter 16 (64 m) for two passes.

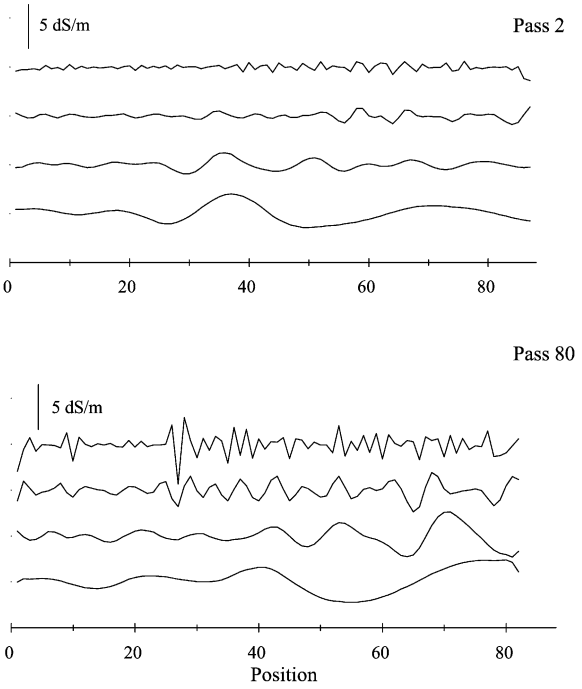

Fig. 11. Detail components for two passes. Detail components for each pass are stacked with scale parameter 16 at the bottom and 2 at the top. The origins of each graph are shifted, the vertical bar shows the scale of the components in dS m^{-1}.

Table 1
Detecting changes in variance for two passes from the EC_a data. The p values were obtained by Monte Carlo analysis

Scale parameter	Segment (positions)	Wavelet variance	Variance ratio	p
Pass 2				
2 (8 m)	3–35	0.04		
	36–88	0.145	4.06	$p < 0.001$
4 (16 m)	5–27	0.04		
	28–88	0.23	5.67	$p < 0.001$
8 (32 m)	1–23	0.112		
	24–88	0.641	5.71	$p < 0.01$
16 (64 m)	1–34	2.15		
	35–88	0.7	3.06	$p > 0.05$
Pass 80				
2 (8 m)	3–23	0.41		
	24–82	1.83	4.44	$p < 0.01$
4 (16 m)	5–21	0.33		
	22–82	1.3	3.84	$p < 0.05$
8 (32 m)	1–58	0.59		
	59–82	4.46	7.5	$p < 0.001$
16 (64 m)	1–62	0.45		
	63–82	1.74	3.89	$p > 0.05$

variable for kriging with external drift (Goovaerts, 1997).

In Section 1 it was noted that one approach to the analysis of data which cannot be assumed to arise from a stationary process is to conduct conventional geostatistical analysis within a local window (Walter et al., 2001). Both wavelet analysis and this approach will require large data sets, and both provide an approach for filtering spatial data into components of different scale which might then be used for further inference or prediction. Odeh and McBratney (2000) illustrate how the local geostatistical analysis might be used in this way.

The particular advantage of the local geostatistical analysis is its flexibility. A local variogram can be computed from data which are regularly distributed in a local window or irregularly distributed. By contrast the standard wavelet analysis used in this paper requires regularly spaced data. Wavelet methods can be applied to data from spatially irregular sample points (Daubechies et al., 1999) but these wavelets cannot be translates or dilates of a basic function so do not generate a MRA comparable to that obtained for our data in this paper.

The particular advantage of wavelet analysis over local geostatistical analysis is a fundamental one, and has been recognised in signal analysis where windowing is used to generate a localized analysis, e.g. by the windowed Fourier transform (Kumar and Foufoula-Georgiou, 1994). In windowed Fourier analysis or localized geostatistical analysis a conventional analysis is conducted on data within a specified local window. We estimate, for example, the variogram of the data for a range of lag intervals from those data within the fixed window. It is clear that the choice of window will have consequences for the results. At any lag close to or larger than the radius of the window the estimated variogram will be subject to edge effects. At shorter lags the variogram may be well estimated, but it will be poorly localized. The estimate will be largely derived from pairs of observations which are some distance from the centre of the window. In summary at most lags the window size will be poorly adapted to a localized geostatistical analysis unless we have some prior information to suggest that the underlying process is stationary within a particular neighbourhood over all spatial scales. In wavelet analysis, by contrast, the wavelet coefficient is estimated from within a scale-specific window since the underlying wavelet function is obtained by a dilation of the basic wavelet. The estimation window is therefore adapted to the scale of interest. This adaptive property of wavelet analysis has been widely recognised as an advantage over windowing methods (Kumar and Foufoula-Georgiou, 1994).

To conclude, wavelet analysis shows that the variation of EC_a data may be very complex and not directly compatible with simple assumptions of statistical stationarity. MRA allows us to explore this complexity within the framework of a coherent mathematical analysis of the data which imposes no assumptions beyond that of finite variance. This may give insight into the data. It may also help in the practical problem of extracting most information from the data for the purpose of predicting soil properties from limited calibration data.

Table 2
Results for maximum likelihood regression of soil properties ρ (bulk density) (g cm^{-3}), θ (volumetric water content) (cm^3 cm^{-3}) and EC_e (electrical conductivity) (dS m^{-1}). Predictors are smooth representations at scale parameter 16 or 8 (P_{16}, P_8) and detail component at scale parameter 16 (Q_{16})

Soil property, depth	Predictor(s)	Error variance	Wald statistic	p*	a[a]
ρ, 30 cm	EC_a	8.59×10^{-3}	5.20	0.023	−189.50
	P_{16}	7.82×10^{-3}	10.09	0.001	**−193.66**
	P_8	8.45×10^{-3}	5.87	0.015	−190.05
	P_{16}, Q_{16}	7.47×10^{-3}	12.63	0.002	−193.64
θ, 30 cm	EC_a	3.37×10^{-3}	2.41	0.12	−231.47
	P_{16}	3.71×10^{-3}	0.05	0.83	−229.28
	P_8	3.29×10^{-3}	2.11	0.35	−231.00
	P_{16}, Q_{16}	3.26×10^{-3}	11.66	0.003	**−236.82**
EC_e, 30 cm	EC_a	77.6	0.001	0.97	149.49
	P_{16}	78.42	2.02	0.16	147.53
	P_8	77.35	0.12	0.73	149.4
	P_{16}, Q_{16}	74.32	7.82	0.02	**144.43**
ρ, 60 cm	EC_a	8.54×10^{-3}	4.70	0.030	−190.01
	P_{16}	8.69×10^{-3}	4.89	0.027	**−190.05**
	P_8	8.84×10^{-3}	3.53	0.06	−188.9
	P_{16}, Q_{16}	8.65×10^{-3}	5.08	0.079	−188.21
θ, 60 cm	EC_a	1.98×10^{-3}	2.95	0.086	−256.86
	P_{16}	2.08×10^{-3}	1.95	0.162	−256.01
	P_8	1.94×10^{-3}	3.42	0.06	−257.2
	P_{16}, Q_{16}	1.87×10^{-3}	3.97	0.137	−255.62
EC_e, 60 cm	EC_a	19.69	13.80	<0.001	117.80
	P_{16}	19.01	13.43	<0.001	119.32
	P_8	17.80	17.34	<0.001	**115.65**
	P_{16}, Q_{16}	17.84	17.84	<0.001	117.04
ρ, 90 cm	EC_a	1.50×10^{-2}	0.005	0.94	−160.90
	P_{16}	1.50×10^{-2}	0.511	0.47	**−161.40**
	P_8	1.51×10^{-2}	0.08	0.77	−161.0
	P_{16}, Q_{16}	1.43×10^{-2}	1.58	0.45	−160.44
θ, 90 cm	EC_a	1.92×10^{-3}	9.51	0.002	**−238.71**
	P_{16}	2.56×10^{-3}	3.20	0.073	−235.33
	P_8	2.25×10^{-3}	6.25	0.012	−237.4
	P_{16},Q_{16}	2.16×10^{-3}	7.25	0.027	−236.01
EC_e, 90 cm	EC_a	25.4	34.04	<0.001	116.48
	P_{16}	19.3	43.68	<0.001	113.34
	P_8	19.1	53.56	<0.001	108.82
	P_{16},Q_{16}	19.1	54.26	<0.001	**110.66**
ρ, 120 cm	EC_a	1.7×10^{-2}	13.1	<0.001	−126.6
	P_{16}	1.8×10^{-2}	13.2	<0.001	−126.7
	P_8	1.7×10^{-2}	15.8	<0.001	**−128.5**
	P_{16}, Q_{16}	1.7×10^{-2}	15.9	<0.001	−126.6
θ, 120 cm	EC_a	2.3×10^{-3}	1.19	0.28	−192.6
	P_{16}	2.4×10^{-3}	0.04	0.84	−191.5
	P_8	2.3×10^{-3}	0.51	0.48	−191.9
	P_{16}, Q_{16}	2.1×10^{-3}	3.13	0.21	−192.5

Table 2 (*continued*)

Soil property, depth	Predictor(s)	Error variance	Wald statistic	p*	a[a]
EC_e, 120 cm	EC_a	72.9	30.9	<0.001	117.6
	P_{16}	48.1	15.6	<0.001	122.4
	P_8	56.6	40.0	<0.001	112.7
	P_{16},Q_{16}	49.9	44.8	<0.001	**112.3**

*p value for the Wald statistic, the null hypothesis is that the predictors are randomly related to the soil property.

[a] Variable part of the Akaike Information Criterion as described in Eq. (17). The values for the four regressions for any one soil property are comparable and a is shown in bold for the regression with the smallest AIC where significant regressions are obtained.

Acknowledgements

The authors wish to acknowledge the University of California Kearney Foundation of Soil Science for the funds that supported the purchase of field instrumentation and funded the chemical analyses for the soil quality assessment, and the University of California Salinity-Drainage program for additional financial support for site preparation and for costs associated with sample collection and site management. Ceil Howe Jr, and Ceil Howe III provided the site and substantial amounts of labour and the use of equipment to help prepare and manage the site. The authors thank Nahid Vishteh and Harry Forster for their analytical technical support and Scott Lesch for his assistance with soil sample design. Finally, the authors acknowledge the conscientious work and diligence of Clay Wilkinson, Derrick Lai, Jon Edwards, and Samantha Chang, who performed the physical and chemical analysis of the soil samples.

RML's work for this paper was supported by the Biological and Biotechnological Science Research Council of the United Kingdom through its grant to Silsoe Research Institute.

References

Abry, P., Goncalves, P., Flandrin, P., 1995. Wavelets, spectrum analysis and 1/*f* processes. In: Antoniadis, A., Oppenheim, G. (Eds.), Lecture Notes in Statistics, Number 103: Wavelets and Statistics, Springer, New York, pp. 15–29.

Burgess, T.M., Webster, R., 1980. Optimal interpolation and isarithmic mapping of soil properties. I. The semivariogram and punctual kriging. Journal of Soil Science 31, 315–331.

Carter, L.M., Rhoades, J.D., Chesson, J.H., 1993. Mechanization of soil salinity assessment for mapping. Proceedings of the 1993 ASAE Winter Meetings, Chicago, IL December.

Cohen, A., Daubechies, I., Vial, P., 1993. Wavelets on the interval and fast wavelet transforms. Applied and Computational Harmonic Analysis 1, 54–81.

Coifman, R.R., Donoho, D.L., 1995. Translation-invariant denoising. In: Antoniadis, A., Oppenheim, G. (Eds.), Lecture Notes in Statistics, Number 103: Wavelets and Statistics, Springer, New York, pp. 125–150.

Cook, D.G., Pocock, S.J., 1983. Multiple regression in geographical mortality studies with allowance for spatially correlated errors. Biometrics 39, 361–371.

Corwin, D.L., Lesch, S.M., 2002. Application of soil electrical conductivity to precision agriculture: theory, principles, and guidelines. Agronomy Journal in press.

Corwin, D.L., Kaffka, S.R., Oster, J.D., Hopmans, J., Mori, Y., van Groenigen, J.-W., van Kessel, C., Lesch, S.M., 2002. Assessment and field-scale mapping of soil quality and hydrologic characteristics of saline-sodic soil. Submitted for publication.

Daubechies, I., 1988. Orthonormal bases of compactly supported wavelets. Communications in Pure and Applied Mathematics 41, 909–996.

Daubechies, I., 1992. Ten Lectures on Wavelets, Society for Industrial and Applied Mathematics (SIAM), Philadelphia.

Daubechies, I., Guskov, I., Schröder, P., Sweldens, W., 1999. Wavelets on irregular point sets. Philosophical Transactions of Royal Society of London, Series A 357, 2397–2413.

Goovaerts, P., 1997. Geostatistics for Natural Resources Evaluation, Oxford University Press, New York.

Goovaerts, P., Webster, R., 1994. Scale-dependent correlation between topsoil copper and cobalt concentrations in Scotland. European Journal of Soil Science 45, 79–95.

Kumar, P., Foufoula-Georgiou, E., 1994. Wavelet analysis in geophysics: an introduction. In: Foufoula-Georgiou, E., Kumar, P. (Eds.), Wavelets in Geophysics, Academic Press, New York, pp. 1–43.

Lark, R.M., 2000. Regression analysis with spatially autocorrelated error: examples with simulated data and from mapping of soil organic matter content. International Journal of Geographical Information Science 14, 247–264.

Lark, R.M., Webster, R., 1999. Analysis and elucidation of soil variation using wavelets. European Journal of Soil Science 50, 185–206.

Lark, R.M., Webster, R., 2001. Changes in variance and correlation of soil properties with scale and location: analysis using an adapted maximal overlap discrete wavelet transform. European Journal of Soil Science 52, 547–562.

Lesch, S.M., Strauss, D.J., Rhoades, J.D., 1995. Spatial prediction of soil-salinity using electromagnetic induction techniques. 2. An efficient spatial sampling algorithm suitable for multiple linear-regression model identification and estimation. Water Resources Research 31, 387–398.

Mallat, S.G., 1989. A theory for multiresolution signal decomposition: the wavelet representation. IEEE Transactions on Pattern Analysis and Machine Intelligence 11, 674–693.

McNeil, J.D., 1992. Rapid, accurate mapping of soil salinity by electromagnetic ground conductivity meters. SSSA Special Publication 30, 201–229.ASA-CSSA-SSSA, Madison, WI.

Odeh, I.O.A., McBratney, A.B., 2000. Using AVHRR images for spatial prediction of clay content in the lower Namoi valley of eastern Australia. Geoderma 97, 237–254.

Oliver, M.A., Webster, R., Slocum, K., 2000. Filtering SPOT imagery by kriging analysis. International Journal of Remote Sensing 21, 735–752.

Percival, D.P., 1995. On estimation of the wavelet variance. Biometrika 82, 619–631.

Percival, D.B., Guttorp, P., 1994. Long-memory processes, the Allan variance and wavelets. In: Foufoula-Georgiou, E., Kumar, P. (Eds.), Wavelets in Geophysics, Academic Press, New York, pp. 325–344.

Press, W.H., Teukolsky, S.A., Vetterling, W.T., Flannery, B.P., 1992. Numerical Recipes (Fortran), 2nd ed, Cambridge University Press, Cambridge.

Rhoades, J.D., 1992. Instrumental field methods of salinity appraisal. SSSA Special Publication 30, 231–248.ASA-CSSA-SSSA, Madison, WI.

Rhoades, J.D., 1993. Electrical conductivity methods for measuring and mapping soil salinity. In: Sparks, D.L., (Ed.), Advances in Agronomy, vol. 49. Academic Press, San Diego, CA, pp. 201–205.

Rhoades, J.D., Corwin, D.L., Lesch, S.M., 1999. Geospatial measurements of soil electrical conductivity to assess soil salinity and diffuse salt loading from irrigation. In: Corwin, D.L., Loague, K., Ellsworth, T.R. (Eds.), Assessment of Non-point Source Pollution in the Vadose Zone, AGU Geophysical Monograph 108, American Geophysical Union, Washington, DC, pp. 197–215.

Voltz, M., Webster, R., 1990. A comparison of kriging, cubic splines and classification for predicting soil properties from sample data. Journal of Soil Science 41, 473–490.

Walter, C., McBratney, A.B., Douaoui, A., Minasny, B., 2001. Spatial prediction of topsoil salinity in the Chelif valley, Algeria using ordinary kriging with local variograms versus a whole-area variogram. Australian Journal of Soil Research 39, 259–272.

Webster, R., Oliver, M.A., 2001. Geostatistics for Environmental Scientists, Wiley, Chichester.

Whitcher, B.J., Guttorp, P., Percival, D.B., 2000. Wavelet analysis of covariance with application to atmospheric time series. Journal of Geophysical Research—Atmospheres 105 (D11), 14941–14962.